Journal of Applied Mechanics and Technical Physics, Vol. 39, No. 3, 1998

ON THE PROBLEM OF CONTROLLING THE EFFICIENCY OF ACTION OF SHAPED-CHARGE JETS

S. V. Demidkov

UDC 531.58:537.634

It is suggested that noncontact action of a magnetic field on shaped-charge jet elements be used to decrease the penetration depth. A decrease in the depth is attained. A physicomathematical model for the process is constructed that allows one to optimize performance of devices used to realize the action of an external magnetic field.

According to hydrodynamical theory [1], the depth of penetration of a shaped-charge jet (SCJ) into a target is $L = l\sqrt{\rho/\rho_1}$, where l is the length of the jet, ρ is the density of the jet material, and ρ_1 is the density of the target material. Hence, ultimately, the SCJ penetration depth is always controlled by changing the SCJ length and density.

Methods of electrodynamics have been successfully used [2–4] to influence a SCJ in the stage of stretching. Shvetsov and Matrosov [2] and Babkin et al. [3] attained a decrease in the penetrating power of a SCJ by speeding up jet breakup and decreasing the jet density by passage of a current pulse through the jet. Fedorov et al. [4] decreased the penetrating power of a SCJ by stretching it in a longitudinal magnetic field.

In the present work, in addition to [2–4], it is suggested that noncontact action of an external magnetic field on a SCJ be used to decrease the penetration depth in the stage where a SCJ is a flow of separate elements. As is known, elongated conducting ($\sigma \not\equiv 0$) magnetic ($\mu \not\equiv 1$) bodies in a magnetic field can orient along the magnetic-field lines [5]. Therefore, if a SCJ element moves at an angle to the magnetic-field line, rotation of the element axis through a certain angle β decreases the element length l_1 in the direction of motion of the center of mass of the element (it is assumed that the element has an elliptic shape and its sections work independently during penetration):

$$l_1 = l_0/\sqrt{\cos^2\beta + (l_0/d)^2\sin^2\beta}.$$

Here l_0 is the length of the element in the direction of the principal axis and d is the diameter of the element.

Calculations show that for elements for which $l_0/d \in [4;\, 8]$, rotation angles of about 15–25° are required to decrease the penetration depth ($l_1/l_0 = 0.5$) by a factor of two. It is therefore of interest to study this mechanism in detail.

We investigate the dynamics of a SCJ element in a homogeneous magnetic field. In the definition of the force moment acting on the element, we assume that the SCJ element has a cylindrical shape.

We consider the cylinder conducting ($\sigma \not\equiv 0$) and magnetic ($\mu \not\equiv 1$). The cylinder axis is located at angle θ to the magnetic-induction vector $\mathbf{B}_1$. The cylinder is elongated $R \ll l_0$ (R and l_0 are the radius and length of the cylinder). We assume that $\mathbf{B}_1$ varies with time by a harmonic law $e^{-i\omega t}$. It is suggested that there is a linear relationship between the magnetization of the cylinder material and the magnetizing field and the quasistaionarity condition is satisfied.

Lykov Academic Scientific Complex "Institute of Heat and Mass Exchange," Minsk 220072. Translated from Prikladnaya Mekhanika i Tekhnicheskaya Fizika, Vol. 39, No. 3, pp. 36–43, May–June, 1998. Original article submitted November 13, 1995; revision submitted September 13, 1996.

0021-8944/98/3903-0355 $20.00 © 1999 Kluwer Academic/Plenum Publishers

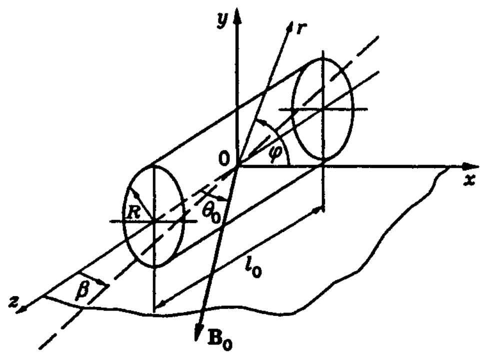

Fig. 1

The system of equations for the rotational motion of a solid body in fixed coordinates x, y, and z (r, φ, and z are fixed cylindrical coordinates, respectively) (Fig. 1) has the form [5]

$$\nabla \times \mathbf{E} = -\frac{\partial \mathbf{B}}{\partial t}; \tag{1}$$

$$\nabla \times \mathbf{H} = \mathbf{j}; \tag{2}$$

$$\mathbf{j} = \sigma(\mathbf{E} + (\omega_1 \times \mathbf{r}) \times \mathbf{B}); \tag{3}$$

$$\mathbf{B} = \mu\mu_0\mathbf{H}; \tag{4}$$

$$\mathbf{I} = (\mu - 1)\mathbf{H}; \tag{5}$$

$$\frac{\partial \mathbf{L}}{\partial t} = \mathbf{K}; \tag{6}$$

$$\mathbf{L} = \int\limits_v \rho(\mathbf{r} \times (\omega_1 \times \mathbf{r}))\,dv; \tag{7}$$

$$\mathbf{K} = \int\limits_v (\mathbf{r} \times ((\mathbf{j} + \mathbf{j}_m) \times \mathbf{B}))\,dv; \tag{8}$$

$$\mathbf{j}_m = \nabla \times \mathbf{I}, \tag{9}$$

where $\mathbf{H}$ and $\mathbf{B}$ are the magnetic-field intensity and induction, $\mathbf{E}$ is the electric-field intensity, $\mathbf{j}$ and $\mathbf{j}_m$ are the densities of the conduction currents and magnetic field, $\mathbf{I}$ is the magnetization of the material, $\mathbf{L}$ is the angular momentum of the cylinder with respect to the center of the fixed coordinate system, $\mathbf{K}$ is the force moment acting on the cylinder, ρ is the density of the cylinder material, v is the volume of the cylinder, ω_1 is the angular velocity of rotation of the cylinder, μ_0 is the magnetic constant, and $\mathbf{r}$ is the radius vector of an arbitrary point of the body. The magnetic field of the source is homogeneous:

$$\mathbf{H}_1 = \{H_{0x}, 0, H_{0z}\}e^{i\omega t}, \quad -\infty < t < \infty.$$

The boundary conditions on the surface of the cylinder are written as

$$\mathbf{B}_n^i = \mathbf{B}_n^e, \tag{10}$$

$$\mathbf{H}_\tau^i = \mathbf{H}_\tau^e \tag{11}$$

(the superscript i refers to the parameters inside the cylinder and the superscript e refers to the region outside of the cylinder).

The boundary conditions for the kinematic parameters of the rotational motion are

$$\omega_1 = \dot{\beta} = 0.$$

System (1)–(9) is nonlinear because the equations of electrodynamics (1)–(5) and (9) are interrelated with the equations of mechanics (6)–(8). We assume that the rotation of the cylinder proceeds rather slowly ($\omega_1 \ll \omega$). Then, (3) takes the form

$$\mathbf{j} = \sigma \mathbf{E}. \tag{12}$$

In this case, system (1), (2), (4), and (12) becomes linear and describes the diffusion of the magnetic field into the fixed cylinder. The force moment (8) is determined using the magnetic-field distribution obtained by solution of system (1), (2), (4), and (12). Since $l_0 \gg R$, the dependence of the magnetic-field parameters on the z coordinate is ignored.

Then, the initial three-dimensional diffusion problem breaks up into two independent problems: a two-dimensional problem for the transverse component of the magnetic-field-intensity vector (the plane xy) and a one-dimensional problem for the longitudinal component H_z.

To determine the transverse component of the intensity vector, it is expedient to introduce the vector magnetic potential $\mathbf{A}$ [6]:

$$\mathbf{H} = \nabla \times \mathbf{A}. \tag{13}$$

Here $\mathbf{A} = \mathbf{A}(r, \varphi, z)$ is a vector that satisfies the calibration ratio [6] $\nabla \mathbf{A} = 0$.

Since the magnetic field of the source varies as $e^{i\omega t}$, by virtue of boundary conditions (10) and (11), the vector magnetic potential $\mathbf{A}$ should be sought in the form

$$\mathbf{A}(r, \varphi, t) = \mathbf{A}_1(r, \varphi) e^{-i\omega t}. \tag{14}$$

Combining (1), (2), (4), and (12)–(14) we arrive at the vector Helmholtz equation:

$$\Delta \mathbf{A} + \mu\mu_0\sigma\omega i \mathbf{A} = 0. \tag{15}$$

Since, by convention, $\mathbf{A}$ defines the transverse component of the vector $\mathbf{H}$, $\mathbf{A}$ is an axial vector. Then (15) reduces to the scalar Helmholtz equation

$$\Delta A_1 + \mu\mu_0\sigma\omega i A_1 = 0. \tag{16}$$

The solution of (16) that satisfies the physical condition of boundedness on the axis ($r = 0$) has the form

$$A_1 = C J_1(kr) \sin\varphi. \tag{17}$$

Here C is a constant and $J_1(kr)$ is a first-order Bessel function of the first kind.

The magnetic field of the reaction $\mathbf{H}_2^{(e)}$ is nonvortex and, hence, satisfies the Laplace equation [6]

$$\Delta\psi = 0, \tag{18}$$

where ψ is the scalar potential of the reaction field;

$$\mathbf{H}_2 = -\nabla\psi. \tag{19}$$

The solution of (18) is written as

$$\psi = C_1 \frac{\cos\varphi}{r} e^{-i\omega t}$$

(C_1 is a constant). Boundary conditions (10) and (11) lead to a system of equations for C and C_1. Solving this system we obtain

$$C_1 = \left(\left((\mu+1)\frac{J_1(kR)}{kRJ_0(kR)} - 1\right) \Big/ \left(1 - (\mu-1)\frac{J_1(kR)}{kRJ_0(kR)}\right)\right) H_0 \sin\theta,$$

$$C = \left(2 \Big/ kJ_0(kR)\left(1 + (\mu-1)\frac{J_1(kR)}{kRJ_0(kR)}\right)\right) H_0 \sin\theta,$$

where $J_0(kR)$ is a zero-order Bessel function of the first kind.

Comparison of (19) with the expression for the intensity vector of the magnetic dipole [6] yields the vector components of the transverse magnetic moment for the cylinder of unit length:

$$m_r = 2\pi R^2 \left(\left((\mu+1) \frac{J_1(kR)}{kRJ_0(kR)} - 1 \right) \Big/ \left(1 + (\mu - 1) \frac{J_1(kR)}{kRJ_0(kR)} \right) \right) H_0 \cos\varphi \sin\theta e^{-i\omega t},$$

$$m_\varphi = -2\pi R^2 \left(\left((\mu+1) \frac{J_1(kR)}{kRJ_0(kR)} - 1 \right) \Big/ \left(1 + (\mu - 1) \frac{J_1(kR)}{kRJ_0(kR)} \right) \right) H_0 \sin\varphi \sin\theta e^{-i\omega t}.$$

Converting to Cartesian coordinates, we obtain

$$m_y = 0, \quad m_x = 2\pi R^2 \left(\left((\mu+1) \frac{J_1(kR)}{kRJ_0(kR)} - 1 \right) \Big/ \left(1 + (\mu - 1) \frac{J_1(kR)}{kRJ_0(kR)} \right) \right) H_0 \sin\theta e^{-i\omega t}. \tag{20}$$

The diffusion of the longitudinal component of the intensity vector is described by the scalar Helmholtz equation [6]

$$\Delta H_z^{(i)} + \mu\mu_0\sigma i H_z^{(i)} = 0. \tag{21}$$

The conditions on the boundary of the cylinder are

$$H_z^{(i)}\Big|_{r=R} = H_{0z} e^{-i\omega t}.$$

The solution of (21) has the form [6]

$$H_z^{(i)} = \frac{J_0(kr)}{J_0(kR)} H_0 \cos\theta e^{-i\omega t}.$$

Using the definition of the magnetic moment [6],

$$m_z = \frac{1}{2} \int_S (\mathbf{r} \times \mathbf{j}_\varphi)\, dS + \int_S \mathbf{I}_z\, dS,$$

we obtain the following expression for the longitudinal magnetic moment of the cylinder of unit length:

$$m_z = \pi R^2 \left(2\mu \frac{J_1(kR)}{kRJ_0(kR)} - 1 \right) H_0 \cos\theta e^{-i\omega t}. \tag{22}$$

Proceeding from (8), we write an expression for the force moment acting on the body in a homogeneous magnetic field [6]:

$$\mathbf{K} = (\mathbf{M} + \mathbf{M}_m) \times \mathbf{B}_1. \tag{23}$$

Here $\mathbf{M} = (1/2)\int_v (\mathbf{r} \times \mathbf{j})\, dv$ is the magnetic moment of conduction currents and $\mathbf{M}_m = (1/2)\int_v (\mathbf{r} \times \mathbf{j}_m)\, dv$ is the magnetic moment of molecular currents.

Using expressions (20) and (22) and assuming that $\mathbf{M} + \mathbf{M}_m = (\mathbf{m}_x + \mathbf{m}_z)\, l_0$, we have the following expression for the force moment acting on the cylinder:

$$\mathbf{K} = \pi R^2 l_0 \frac{B_0^2}{2\mu_0} \mathrm{Re}\left(\frac{2\mu(\mu-1) - (J_1(kR)/kRJ_0(kR))^2 - (\mu+1)(J_1(kR)/kRJ_0(kR)) + 1}{1 + (\mu-1)(J_1(kR)/kRJ_0(kR))} e^{-i\omega t} \right) \cos\omega t \sin 2\theta \mathbf{e}_y. \tag{24}$$

In extreme cases, the general expression of the force moment (24) can be brought to the form that allows one to perform routine practical calculations.

1. Case of Low Frequencies ($R/\delta \leqslant 1$, where δ is the thickness of a classical skin layer) [6]. Expansion of the Bessel functions J_0 and J_1 in series in the parameter kR [7] yields

$$\mathbf{K} = \frac{B_0^2}{2\mu_0} \pi R^2 l_0 \left(\mu \frac{1 + (1/24)(R/\delta)^4}{1 + (1/8)(R/\delta)^4} \cos\omega t + \mu \frac{(1/4)(R/\delta)^2 + (3/1152)(R/\delta)^6}{1 + (1/8)(R/\delta)^4} \sin\omega t \right) \cos\omega t \sin 2\theta \mathbf{e}_y \tag{25a}$$

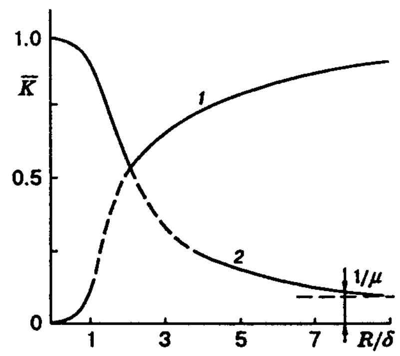

Fig. 2

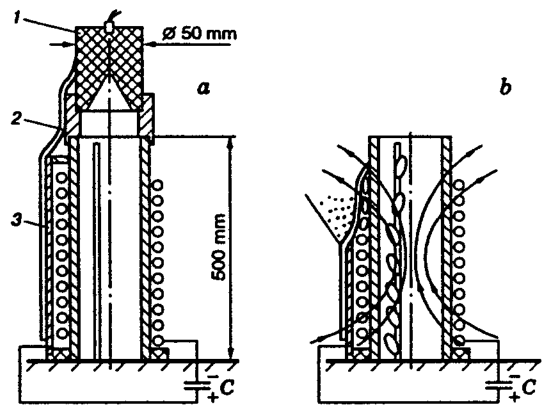

Fig. 3

for $\mu \gg 1$ and

$$\mathbf{K} = \frac{B_0^2}{2\mu_0}\pi R^2 l_0\left(\frac{1}{24}\left(\frac{R}{\delta}\right)^4 \cos\omega t - \frac{1}{4}\left(\frac{R}{\delta}\right)^2 \sin\omega t\right)\cos\omega t \sin 2\theta \mathbf{e}_y \tag{25b}$$

for $\mu = 1$ (which is equivalent to the result obtained in [6]).

2. Case of High Frequencies ($R/\delta > 1$):

$$\mathbf{K} = \frac{B_0^2}{2\mu_0}\pi R^2 l_0\Bigg(\frac{1-(\mu^2/2)(\delta/R)^2+(\mu^3/2)(\delta/R)^3}{1+\mu\delta/R+(\mu^2/2)(\delta/R)^2}\cos\omega t$$
$$+\frac{(\mu^3/2)(\delta/R)^3+\mu^2(\delta/R)^2-\mu\delta/R}{1+\mu\delta/R+(\mu^2/2)(\delta/R)^2}\sin\omega t\Bigg)\cos\omega t \sin 2\theta \mathbf{e}_y \tag{26a}$$

for $\mu \gg 1$ and

$$\mathbf{K} = \frac{B_0^2}{2\mu_0}\pi R^2 l_0\left(\left(1-\frac{\delta}{R}\right)\cos\omega t - \frac{\delta}{R}\sin\omega t\right)\cos\omega t \sin 2\theta \mathbf{e}_y \tag{26b}$$

for $\mu = 1$ (which is equivalent to [6]).

Since the angular frequency of rotation of the cylinder ω_1 is assumed to be far lower than the frequency of variation of the source field, in the equation of rotation it is expedient to use (25) and (26) averaged over the period of fluctuations of the source field $T = 2\pi/\omega$. Figure 2 shows the variation in the acting value of the force moment $\bar{K} = 4\mu_0 K^*/(\mu B_0^2 \pi R^2 h)$ (K^* is the acting value of the force moment) versus the dimensionless parameter R/δ. When the cylinder material shows clearly defined magnetic properties ($\mu \gg 1$) (curve 2 in Fig. 2), the force moment decreases monotonically as the frequency increases (the value of R/δ increases). In the case of a nonmagnetic cylinder, the force moment increases with increase in the frequency, tending, as in the case of $\mu \not\equiv 1$, to the force moment acting on a superconductor of equivalent dimensions and shape (curve 1 in Fig. 2).

Since in explosive experiments, steel SCJ are frequently used, it is impossible to rule out the effects connected with the presence of intrinsic magnetic properties of a SCJ.

In the case of a homogeneous magnetic field, Eq. (6) becomes

$$J\ddot{\beta} = D\sin 2(\theta_0 - \beta), \tag{27}$$

where J is the moment of inertia of the cylinder with respect to the y axis,

$$D = \frac{1}{\omega}\int_0^{2\pi}\mathrm{Re}\left(\frac{(2\mu(\mu-1)(J_1(kR)/kRJ_0(kR))^2-(\mu+1)(J_1(kR)/kRJ_0(kR))+1)\,e^{-i\omega t}}{1+(\mu-1)(J_1(kR)/kRJ_0(kR))}\right)d\omega t\,\frac{B_0^2}{2\mu_0}\pi R^2 l_0,$$

and β is the current rotation angle of the cylinder. When the angle β is small ($\beta \ll \theta_0$) and the initial

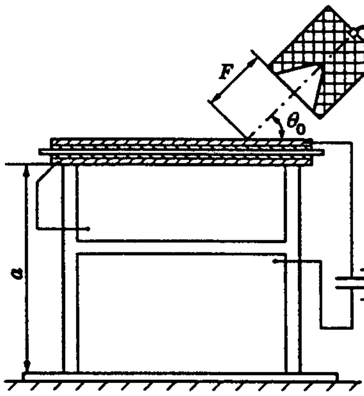

Fig. 4

TABLE 1

U_0, kV	J_m, kA	$l \cdot 10^{-3}$, m
0	0	60, 60, 70, 65, 65
1.5	65	65, 65
3	109	50, 43, 60, 65
4.2	150	34, 42, 40

Note. $\rho_R = 0.019\ \Omega$, $\theta_0 = 45°$, $C = 1800 \cdot 10^{-6}$ F, $L_1 = 0.232 \cdot 10^{-3}$ H, and $a = 75 \cdot 10^{-3}$ m.

TABLE 2

U_0, kV	J_m, kA	$a \cdot 10^{-3}$, m	$l \cdot 10^{-3}$, m
0	0	50	82, 90, 80
0	0	75	60, 60, 70, 65, 65
4.2	150	50	60, 60, 60
4.2	150	75	34, 42, 40, 30

Note. $\rho_R = 0.019\ \Omega$, $\theta_0 = 45°$, $C = 1800 \cdot 10^{-6}$ F, and $L_1 = 0.232 \cdot 10^{-3}$ H.

TABLE 3

U_0, kV	J_m, kA	θ_0, deg	$l \cdot 10^{-3}$, m
4.2	150	90	75
4.2	150	60	63, 56, 50
0	0	60	75, 80, 75, 80, 60
4.2	150	45	34, 42, 40, 30
0	0	45	60, 60, 70, 65, 65

Note. $\rho_R = 0.019\ \Omega$, $a = 75 \cdot 10^{-3}$ m, $C = 1800 \cdot 10^{-6}$ F, and $L_1 = 0.232 \cdot 10^{-3}$ H.

conditions for the kinematic parameters are zero, from (27) for the time of the rotation angle, we obtain $t = \sqrt{2\beta J/D \sin 2\theta_0}$.

Noncontact action was realized by means of a multiturn solenoid (Fig. 3a). The multiturn solenoid operated as follows. During passage of a detonation wave through the charge 1, detonation is transferred to the strip 2 of an elastic explosive which throws mobile contact 3 of the discharge circuit. As a result, the discharge circuit is completed, and the capacitor bank discharges into the solenoid. A magnetic field is produced inside the solenoid. A steel pipe with wall thickness $3 \cdot 10^{-3}$ m having a groove along the generatrix for free penetration of the magnetic field in the solenoid space was placed inside the solenoid to preserve the geometry of the working space. During passage of a SCJ through the solenoid space, because of the curvature of the force lines at the edges of the solenoid, the jet elements are acted upon by a force moment that tends to rotate the elements through certain angles with respect to the axis of motion of their centers of mass. For an initial energy of the capacitor bank $W_0 = 1.25$ kJ, the depths of penetration of SCJ from charges of diameter $5 \cdot 10^{-2}$ m were $(35, 55, 55, 55, 75, 60) \cdot 10^{-3}$ m, and for $W_0 = 0$ (the capacitor bank was disconnected), they were $(100, 175, 160, 130, 96) \cdot 10^{-3}$ m.

Proceeding from (26) and (27), we estimate the rotation angles of SCJ elements under the conditions of the experiment performed. During device operation (Fig. 3b), after attainment of the minimum value of the solenoid inductance $L_k = \mu_0 R_1 \ln(8R_1/d_1 - 7/4)$ [6] (R_1 is the radius of the solenoid turn and d_1 is the wire diameter) the energy of the capacitor bank is concentrated at the bottom of the solenoid in a volume $v_1 \sim 16\pi R_1^3$ (the magnetic-field induction of the turn with a current varies with distance z from its plane as the function $B_z = (\mu_0 I/2)R_1^2/(R_1^2 + z^2)^{3/2}$ [8]). Therefore the time of action of the magnetic field on a jet element $t_{\rm rot}$ is of the order of $4R_1/V$, where V is the rate of motion of the jet element. Hence, during passage through the working space of the solenoid, the rotation angle of the element is

$$\beta' \sim \frac{W_0}{\rho l_0^2 R_1 V^2} \frac{1 - 0.5(\delta/R)^2 + 0.5(\delta/R)^3}{1 + \delta/R + 0.5(\delta/R)^2}, \tag{28}$$

and during motion inside the cavern, it is $\beta'' \sim \beta' L/(2R_1)$. The total rotation angle is $\beta = \beta' + \beta''$.

For the characteristic parameters (element $\mu \equiv 1$, a copper jet, $V \in [3; 5] \cdot 10^3$ m/sec, $l_0 = 8 \cdot 10^{-3}$ m, and $\delta \in [0.5; 0.7] \cdot 10^{-3}$ m) at $W_0 = 1.25$ kJ, we obtain $\beta \in [2.5; 6°]$, which is similar in order of magnitude to the angles required for a twofold decrease in the SCJ penetration depth ($\beta \in [12; 25°]$). In this case, from (28) it follows that when the general magnetic energy in the working space is constant, an increase in the magnetic-energy density enhances the effect of the external magnetic field on the SCJ.

Experiments on the action on SCJ were also performed under conditions where a magnetic field was produced in the working volume by a capacitor-bank discharge into a multiturn solenoid (Fig. 4). The experiments were performed with charges of diameter 36 mm. The results of the experiments are presented in Tables 1–3, where L_1 is the total inductance of the discharge circuit, ρ_R is the total ohmic resistance to the discharge circuit, J_m is the amplitude of the current, and U_0 is the voltage.

Thus, the present work shows the possibility of decreasing the SCJ penetration depth under the effect of an external magnetic field. A physicomathematical model is proposed that allows one to optimize parameters of the technical devices used to implement the method.

REFERENCES

1. F. A. Baum, L. P. Orlenko, and K. P. Stanyukovich, *Physics of Explosion* [in Russian[, Nauka, Moscow, (1975).
2. G. A. Shvetsov and A. D. Matrosov, "Current instability of shaped-charge jets," in: *Lavrent'ev Lectures on Mathematics, Mechanics, and Physics*: Abstracts of IV Int. Conf. (Kazan', July 3–7, 1995), Inst. of Hydrodynamics, Novosibirsk (1995), p. 132.
3. A. V. Babkin, M. E. Kolychev, V. A. Kruzhkov, et al. "One possible mechanism of disruption of a shaped-charge jet by a current pulse," *ibid.*, p. 119.
4. S. V. Fedorov, A. V. Babkin, and D. S. Botkin, "Effect of a longitudinal low-frequency magnetic field on the deformation of a shaped-charge jet in free flight," *ibid.*, p. 158.
5. G. Ya. Sermons, *Dynamics of Solid Bodies in an Electromagnetic Field* [in Russian], Zinante, Riga (1974).
6. L. D. Landau and E. M. Lifshits, *Electrodynamics of Continuous Media* [in Russian], Nauka, Moscow (1982).
7. E. Jahnke, F. Emde, and Lõsh, *Tafeln Hhĕrer Funktionen*, Teubuer, Stuttgart (1959).
8. B. L. Alievskii and V. L. Orlov, *Calculation of Magnetic-Field Parameters for Axisymmetric Coils, Handbook* [in Russian], Energoatomizdat, Moscow (1983).